

Electronic Supplementary Information

Tuning the interpenetration of metal–organic frameworks through changing ligand functionality: Effect on gas adsorption properties

Bin Li^a, Qing-Qing Yan^a, Zhi-Qiang Xu^b, Ying-Bo Xu^{b*} and Guo-Ping Yong^{a*}

^a Department of Chemistry, University of Science and Technology of China, Hefei 230026, P. R. China. E-mail: gpyong@ustc.edu.cn

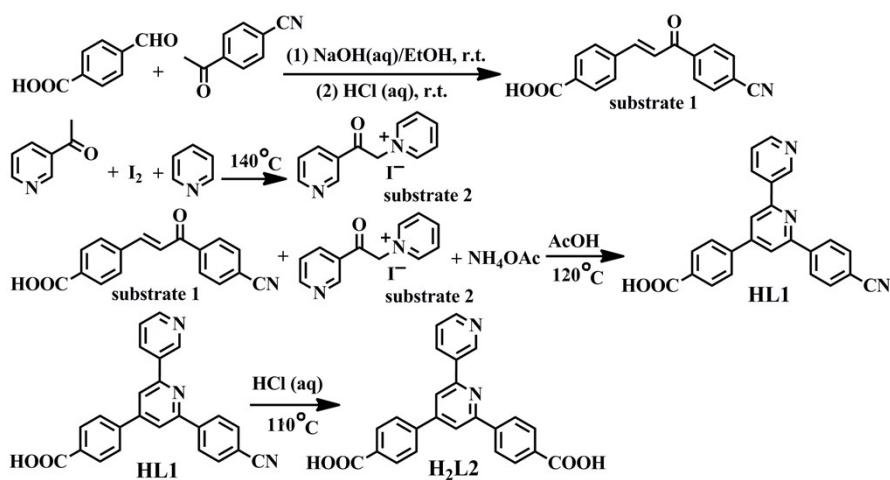
^b The USTC-Anhui Tobacco Joint Laboratory of Chemistry and Combustion, Hefei 230066, P. R. China. E-mail: 838654606@qq.com

Table S1 Selected bond distances (Å) and angles (°) for USTC-2–USTC-4.^a

USTC-2		USTC-3		USTC-4	
Co(1)-O(1)#15	1.991(4)	Zn(1)-O(1)	1.972(5)	Co(1)-O(1)	2.035(3)
Co(1)-O(1)#16	1.991(4)	Zn(1)-O(1)#14	1.972(5)	Co(1)-O(5)	1.975(2)
Co(1)-N(1)	2.051(4)	Zn(1)-N(1)#11	2.058(6)	Co(1)-O(7)#2	2.050(3)
Co(1)-N(1)#14	2.051(4)	Zn(1)-N(1)#12	2.058(6)	Co(1)-O(8)#2	2.349(2)
O(1)#15-Co(1)-O(1)#16	99.9(2)	O(1)-Zn(1)-O(1)#14	105.2(3)	Co(1)-N(4)#4	2.084(3)
O(1)#15-Co(1)-N(1)	116.22(17)	O(1)-Zn(1)-N(1)#11	116.0(2)	Co(2)-O(1)	2.082(2)
O(1)#15-Co(1)-N(1)#14	108.34(17)	O(1)-Zn(1)-N(1)#12	106.9(2)	Co(2)-O(3)#4	2.096(3)
O(1)#16-Co(1)-N(1)	108.34(17)	O(1)#14-Zn(1)-N(1)#11	106.9(2)	Co(2)-O(4)#4	2.157(3)
O(1)#16-Co(1)-N(1)#14	116.22(17)	O(1)#14-Zn(1)-N(1)#12	116.0(2)	Co(1)-O(8)#2	2.191(2)
N(1)-Co(1)-N(1)#14	107.993	N(1)#11-Zn(1)-N(1)#12	106.3(3)	Co(2)-O(9)	2.084(3)
				Co(2)-N(2)#2	2.081(3)
				O(1)-Co(1)-O(5)	115.33(11)
				O(1)-Co(1)-O(7)#2	111.16(10)
				O(1)-Co(1)-O(8)#2	77.18(9)
				O(1)-Co(1)-N(4)#4	109.63(12)
				O(5)-Co(1)-O(7)#2	106.03(10)
				O(5)-Co(1)-O(8)#2	164.03(10)
				O(5)-Co(1)-N(4)#4	97.03(12)
				O(7)#2-Co(1)-O(8)#2	58.71(8)
				O(7)#2-Co(1)-N(4)#4	117.11(12)
				O(8)#2-Co(1)-N(4)#4	87.23(10)
				O(1)-Co(2)-O(3)#4	93.77(10)
				O(1)-Co(2)-O(4)#4	153.29(10)
				O(1)-Co(2)-O(8)#2	79.94(10)
				O(1)-Co(2)-O(9)	102.47(11)
				O(1)-Co(2)-N(2)#2	101.49(11)
				O(3)#4-Co(2)-O(4)#4	61.62(10)
				O(3)#4-Co(2)-O(8)#2	88.31(10)

O(3)#4-Co(2)-O(9)	92.00(11)
O(3)#4-Co(2)-N(2)#2	163.82(12)
O(4)#4-Co(2)-O(8)#2	88.58(10)
O(4)#4-Co(2)-O(9)	89.42(11)
O(4)#4-Co(2)-N(2)#2	102.36(11)
O(8)#2-Co(2)-O(9)	177.54(11)
O(8)#2-Co(2)-N(2)#2	89.10(10)
O(9)-Co(2)-N(2)#2	89.93(12)

^a Symmetry code for **USTC-2**: #14=-x+1/2, -y+1/2, z, #15=x+3/4, -y+3/4, z+1/4, #16=-x+3/4, y+3/4, z+1/4; symmetry code for **USTC-3**: #11=x+3/4, -y+1/4, z+3/4, #12=-x+3/4, y+1/4, z+3/4, #14=-x+1/2, -y+1/2, z; symmetry code for **USTC-4**: #2=-x, y+1/2, -z+1/2, #4=x, -y-1/2, z-1/2.



Scheme S1 The synthesis procedure for HL1 and H₂L2 ligands.

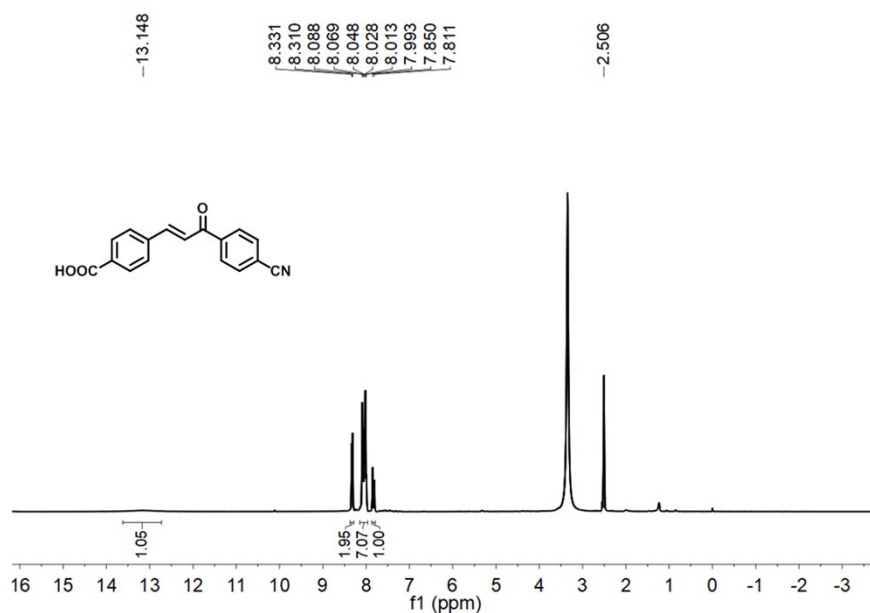


Fig. S1 ¹H NMR (400 MHz, dms-*d*₆) of substrate 1.

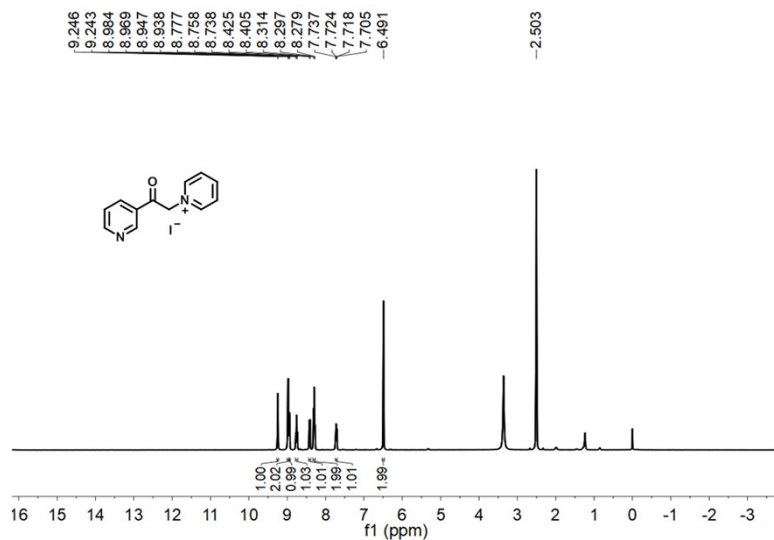


Fig. S2 ^1H NMR (400 MHz, $\text{dms}\text{-}d_6$) of substrate 2.

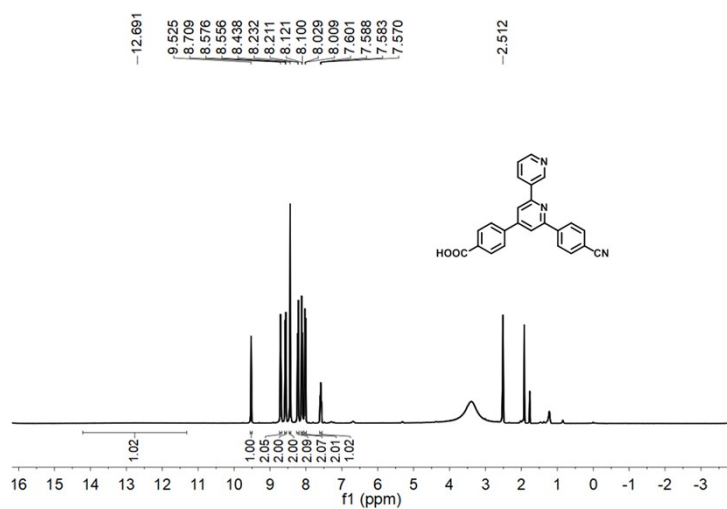


Fig. S3 ^1H NMR (400 MHz, $\text{dms}\text{-}d_6$) of HL1.

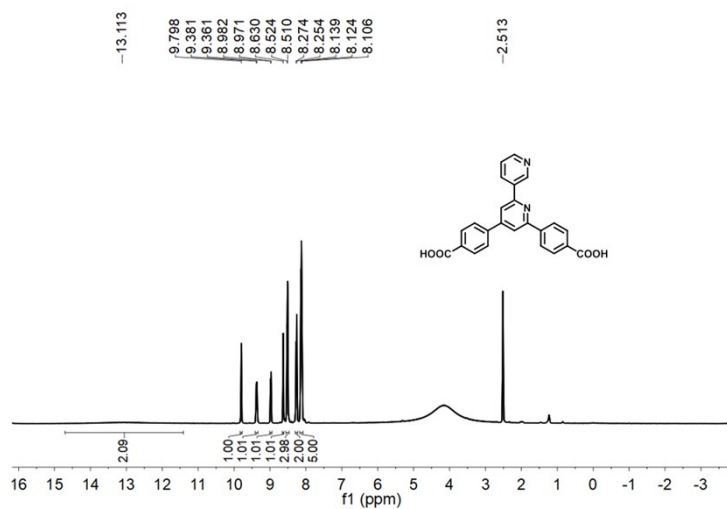


Fig. S4 ^1H NMR (400 MHz, $\text{dms}\text{-}d_6$) of H_2L_2 .

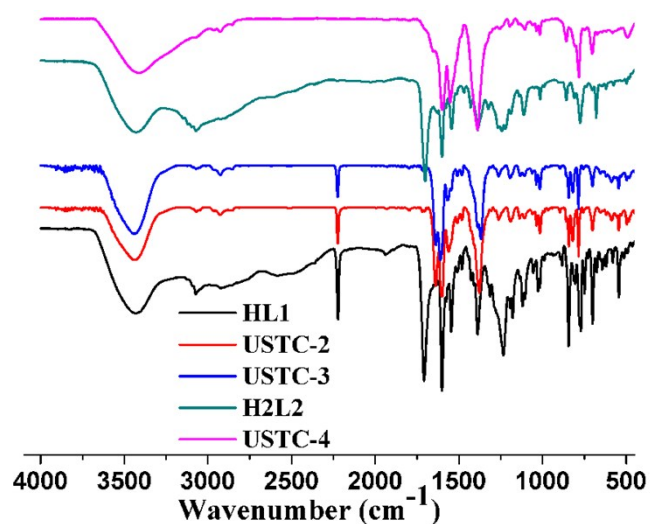


Fig. S5 IR absorption of HL1 and H₂L2 ligand, and USTC-2–USTC-4.

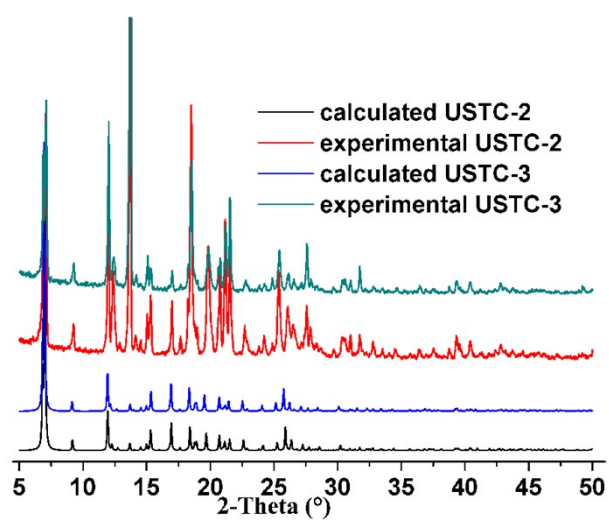


Fig. S6 Powder XRD profiles of USTC-2 and USTC-3.

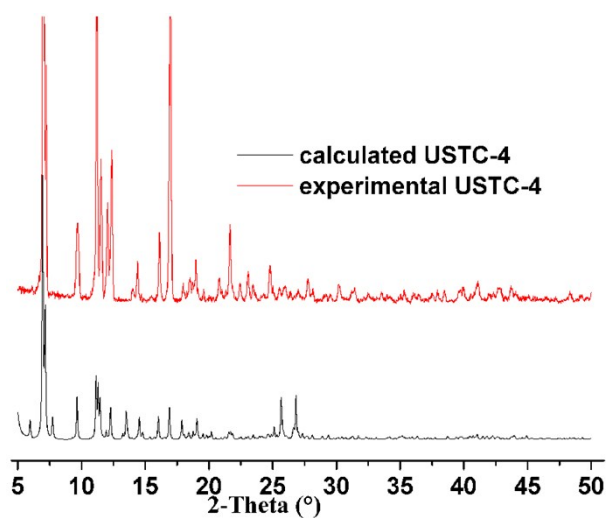


Fig. S7 Powder XRD profiles of USTC-4.

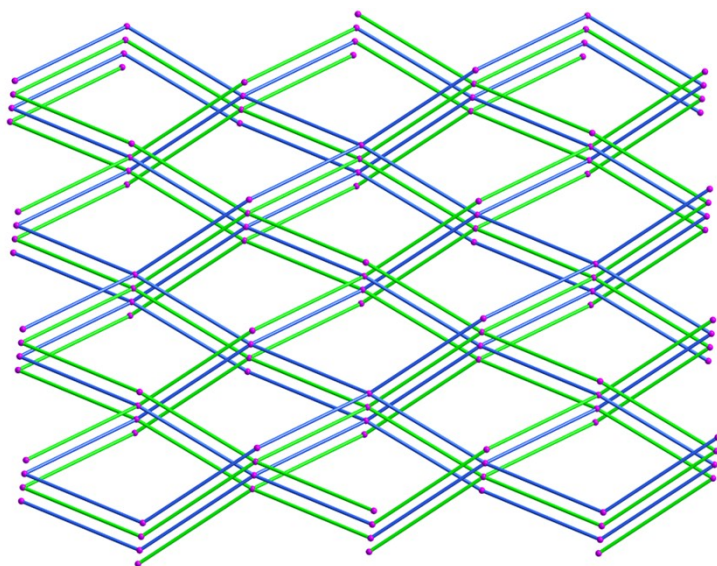


Fig. S8 The two-fold interpenetrated 3D framework of USTC-2.

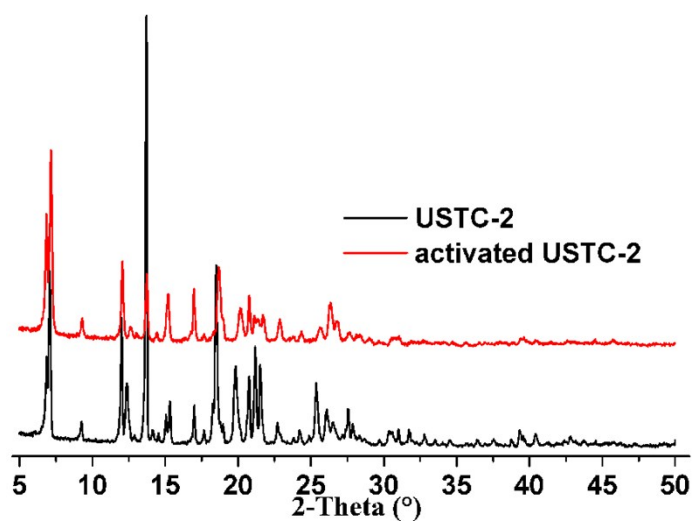


Fig. S9 Powder XRD profiles of USTC-2 and activated USTC-2.

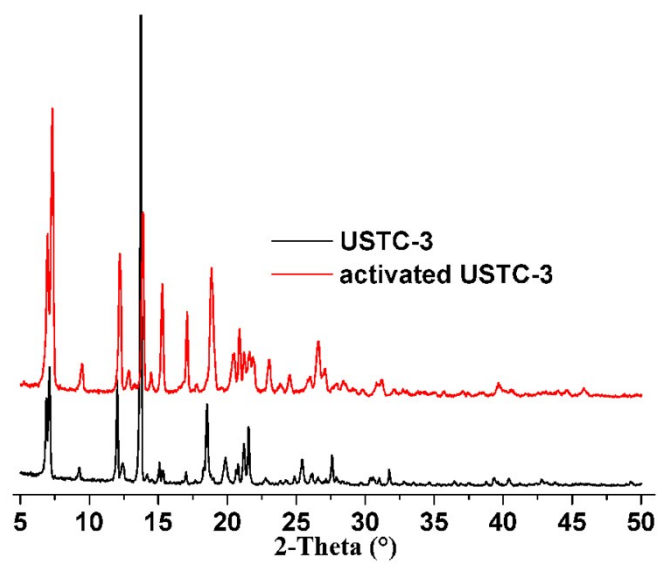


Fig. S10 Powder XRD profiles of USTC-3 and activated USTC-3.

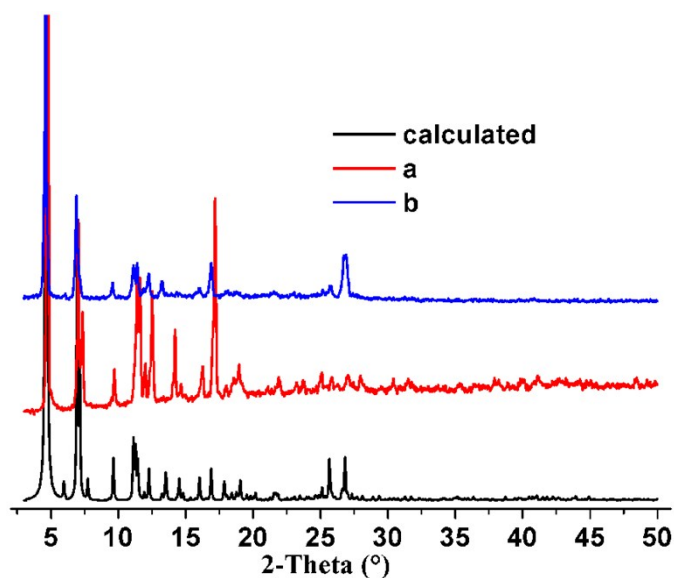


Fig. S11 Powder XRD profiles of USTC-4 (calculated), and activated USTC-4 before (a) and after (b) N₂ adsorption experiment.

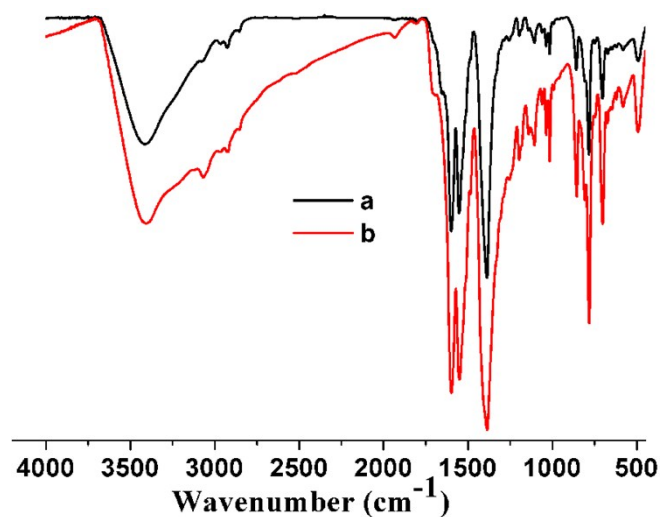


Fig. S12 IR absorption of activated USTC-4 before (a) and after (b) N₂ adsorption experiment.

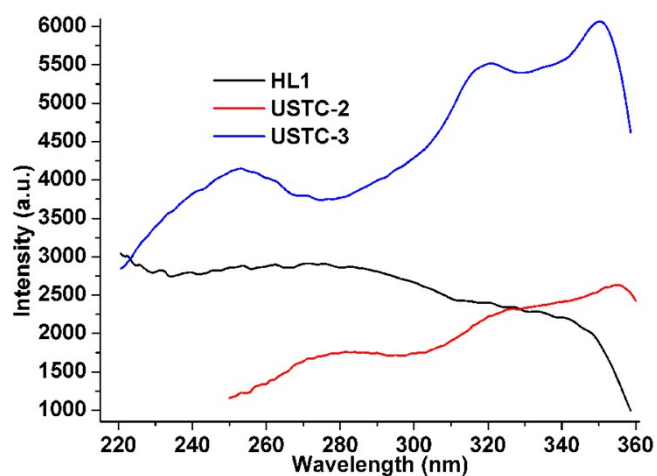


Fig. S13 Solid-state excitation spectra of HL1 ligand, USTC-2 and USTC-3.

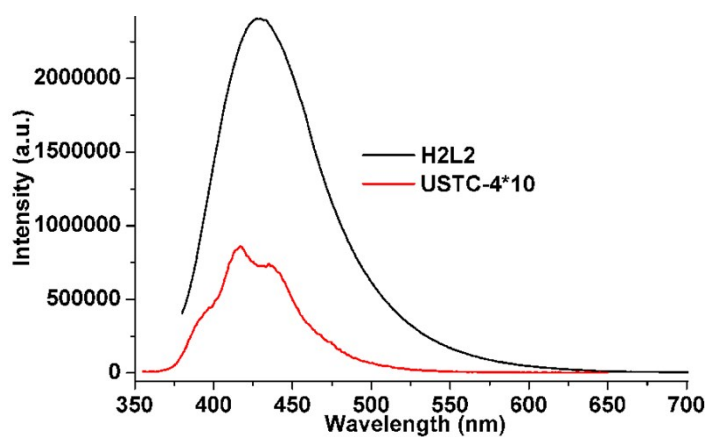


Fig. S14 Solid-state PL spectra of H₂L2 ligand and USTC-4.

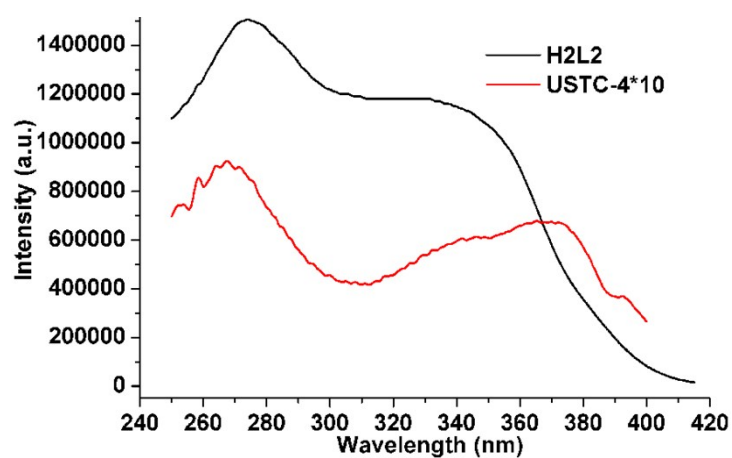


Fig. S15 Solid-state excitation spectra of H₂L2 ligand and USTC-4.